ANTHROPOLOGIE • LIX/1 • pp. 23–34 • 2021

VERONIKA KOVÁČOVÁ, PETRA URBANOVÁ

A NOVEL SEMI-AUTOMATIC MEASUREMENT OF THE SEMICIRCULAR CANALS OF THE HUMAN BONY LABYRINTH

ABSTRACT: The bony labyrinth is an inner ear structure located inside the pyramid of the temporal bone. In skeletal or skeletonized human remains, the region exhibits a remarkably high resistance against a variety of taphonomic factors. A substantial amount of work has been carried out in many scientific domains assessing morphological variations of the bony labyrinth. However, the results of these studies are inconsistent with each other, so researchers remain unable to definitively confirm or reject size and shape dependencies of the bony labyrinth on factors such sex or age. Inadequate methodology and the invasiveness of existing approaches are frequently cited as reasons for these ambiguous results. This paper proposes a new semiautomatic PC-aided approach for quantifying the semicircular canals of the bony labyrinth using CT-generated three-dimensional digital models. A new measurement protocol was established on a sample of 163 bony labyrinths using a step-wise elimination procedure and semi-automatic computer-assisted tools. The procedure finally selected as most effective included 39 measurements, which were employed to explore age, sex or side-to-side differences in the shape and size of the semicircular canals. The results exhibit very few sex-related and body-side-specific differences. However, statistically significant differences were observed between sub-adults and adults, particularly in the canal lumens of the lateral and posterior semicircular canals, where larger values were detected for the adults. This paper presents a novel innovative approach for quantifying the semicircular canals of the bony labyrinth, with the aim of regularizing the methodological pool in this line of research.

KEY WORDS: Human bony labyrinth – CT imaging – 3D digital models – Morphological variation

INTRODUCTION

The human bony labyrinth is a cavernous system enclosed by the layers of highly resistant cortical bone which form the pyramid of the temporal bone. Its primary function is to protect the organs of hearing and balance. Its central part is formed by the vestibule, an egg-shaped cavity with two vestibular sacs on the

Received 12 November 2019; accepted 9 April 2020.

DOI: https://doi.org.10.26720/anthro.20.05.11.1

medial wall, the saccule and the utricle (Dokládal, Páč 2000). Each of the vestibular sacs has an expanded area of wall called the macula. The macula of the saccule and the macula of the utricle are collectively referred to as the acoustic maculae (Dorland 2011). The vestibule extends forward into a snail-shell-like structure – the cochlea. In the opposite direction, the vestibule spreads into three semicircular C-shaped canals, oriented approximately in the perpendicular planes – the lateral semicircular canal, which runs horizontally, the superior semicircular canal, which runs vertically, and the posterior semicircular canal, running in a downward angle. One end of each canal enlarges into a bulbous termination (the loop), while the opposite end is merely an extension with no (or only subtle) modifications in width (Dokládal, Páč 2000). The terminations of the posterior and superior semicircular canals merge into the common crus.

The inner ear structures, embedded inside the thick hard body mass of the pyramid, have traditionally been explored in cadaveric studies using invasive techniques such as histological slices or calcified thin sections (Hardy 1938, Henderson *et al.* 2011). Radiographs were also demonstrated as a possible method for examining the inner ear (Kováčová *et al.* 2016). While the histological approach is irreversible, destructive and time-consuming, X-rays are non-invasive. However, with both methods, the three-dimensional anatomical structures of the bony labyrinth are reduced to a set of two-dimensional representations, which retain very little of their original spatial arrangement inside the pyramid (Weber 2015). Out of this reason, positioning of the scanned bone, and thus the projection plane of the radiographs is crucial for enabling correct, accurate and reproducible assessment, particularly when measurements are also taken (Beckett, Conlouge 2010, Spoor *et al.* 2000)

Recently, extensive development in imaging technologies such as computed tomography (CT), microtomography (μCT) and nanotomography have made it possible to apply a variety of digital examination protocols to studies of anatomical structures (Müller 2009). Such techniques are non-invasive and do not cause damage to the structure or its surroundings (Recheis *et al.* 1999, Weber 2015). Because of increased computing power which can run image processing algorithms rapidly and effectively even on personal computers, the current trend has been to conduct morphological studies on digital models in a virtual environment (Recheis *et al.* 1999). For instance, studies by Gunz *et al.* (2012) and Osipov *et al.* (2013) showed that these techniques could be valuable assets in exploring morphological variations of the bony labyrinth.

Despite the abundance of literature on the human bony labyrinth, the results regarding morphological variations and their intervening factors—such as age, sex, and population affinity—remain contradictory. For instance, Henderson *et al.* (2011) showed that there were no age-related modifications in the maximum diameter of the auditory nerve canal if measured on histological slices from birth to the age of 100. In contrast, utilizing 2D reconstructive methods on a series of sequential sections, Hardy (1938) demonstrated that individuals over 20 years old possessed longer auditory nerve canals and cochlea than younger age groups.

Similarly, the conclusions regarding side differences are not consistent in the existing literature. Although most of the studies (Lee *et al.* 2013, Della Santina *et al.* 2005, Hardy 1938) found no side-specific morphological variations, by contrast, Osipov *et al.* (2013) reported significant asymmetry in multiple dimensions and indices on the semicircular canals, as well as cochlea. Statistically significant asymmetry was demonstrated in heights of all canals, the width of the anterior canal, the height to width index of the posterior canal and some measures for radius of curvature of the anterior and posterior canal. Besides that, they observed statistical side-differences also in the width and the height to width ratio of cochlea.

There have been similar disagreements and ambiguity regarding the presence and extent of sexual dimorphism. Hardy (1938) reported that measurements in males were 3% larger than those in females. Sato *et al.* (1991), employing 3D reconstructed thin-sections, reported sex-related variation of as much as 12.9%. Also, Marcus *et al.* (2013) reported statistical sex-related differences in 4 out of 12 dimensions of the bony labyrinth, ranging from 3.9 to 11.6% (with lower values for females). However, none of the parameters on the semicircular canals were statistically significant. Sato *et al.* (1992) demonstrated that the surface areas of the macula of the saccule and the macula of the utricle were up to approximately 20 to 24% larger in males than in females, and so was the width of the macula of the utricle, the length of the macula of the saccule, and the diameter of the superior semicircular canal, although here the differences were only within an interval from 5 to 12%. On the other hand, the study by Lee *et al.* (2013), which was conducted on three-dimensional reconstructions of micro-CT data,

detected only minimum sexual dimorphism in the dimensions of the semicircular canal lumens.

These inconsistent results, which have made it impossible to confirm or reject dependencies of labyrinth morphology on causative factors, show that our current knowledge of this subject remains insufficient. In explaining this insufficiency, many have stressed the lack of a standardized methodological basis and the invasiveness and the laboriousness of the existing approaches.

The aim of the present study is to formulate a novel procedure for rigorous assessment of the human bony labyrinth, to test its accuracy and efficiency, and finally to apply it in order to explore morphological variations within a sample of human crania.

METHODS

The studied sample consisted of 163 human bony labyrinths in various stages of preservation, embedded in complete crania, fragments of basicrania, or fragments of separate temporal bones. The skeletal remains originated from the early medieval archaeological site Dětkovice – Za zahradama, dated to the 11th to 12th century AD. Biological profiles of the individuals (sex and age) were assessed with a combination of several metric and morphoscopic methods, primarily on the cranium and pelvis for the sex determination, on the pelvis and teeth (dental wear) for the adults' age estimation and the teeth (mineralization and eruption) and postcranial skeleton (fusion of ossification centers, measurements of selected bones) for subadults (for review, see Jungerová *et al.* 2016). When the determination of characteristics was hampered by poor preservation of the skeletal material, individuals were classified as nondefinable (nd). Sex and side distribution of the studied sample is shown in *Table 1*. The age of individuals ranged from 0 to 65, and for the purpose of the study the subjects were grouped into eight age categories, reflecting the developmental and subsequent aging stages (*Table 2*).

In order to visualize the studied inner ear structures, each bone was examined using a cone-beam CT unit (iCAT, Imaging Sciences International, Hatfield, PA) set as follows: slice thickness – 0.125 mm; voltage – kVp 120; field of view – 100 mm × 100 mm; voxel resolution – 0.125 mm; matrix – 1280×1280 px. The CT scans were segmented interactively by employing segmentation functionalities available in AMIRA 5.3.2 software (Visage Imaging, Inc. 2010). For the inner ear cavities, the magic wand segmentation tool was used with a fixed threshold set to 120.

Three-dimensional digital models were built, smoothed with the factor set to 0.6, and saved as "stl" files. In addition, they were checked for errors and hole-filled in the GOM Inspect program (GOM mBH 2013) V8 using the functions "Eliminate Mesh Errors" and "Close Holes" (with very smooth or plane-based patch settings: Max. hole size – 1000 mm; Max. number of edges – 1000; Delete neighborhood – 1). They were then re-smoothed using the Smooth function (filter radius – very large; detail sharpness – very low; surface tolerance – 0.65 mm). In order to

TABLE 1: Sex and side distribution of the sample; dx – dexter, sin – sinister, nd – nondefinable.

Category	**Subadults**		**Adults**				**Nd**	
Number of individuals	86		74				3	
Side	**dx**	**sin**	**dx**		**sin**		**dx**	**sin**
Number of individuals	42	44	35		39		1	2
Category	**Subadults**		**Females**		**Males**		**Nd**	
Number of individuals	86		34		40		3	
Side	**dx**	**sin**	**Dx**	**sin**	**dx**	**sin**	**dx**	**sin**
Number of individuals	42	44	16	18	19	21	1	2

TABLE 2: Number of individuals in the age categories.

Age categories [years]	**0–0.5**	**0.5–1.5**	**1.5–3**	**3–6**	**6–14**	**14–30**	**30–65**	**nd**
Number of individuals	9	15	18	24	11	13	65	8

prevent the possibility of bias and to avoid subjective influence during further processing, all left-sided 3D models were mirrored so that they would correspond to their right-sided counterparts.

Procedure development – proposal, testing and evaluation of several assessment methods

Three separate procedures were proposed to quantify morphological variations in the semicircular canals of the human bony labyrinth. Each of them was tested for accuracy and repeatability. The first procedure was based on the endpoints of selected linear measurements (landmarks) collected manually using the Landmark program (Wiley 2005), while the two other procedures, executed in the GOM Inspect program (GOM mBH 2013), relied on incorporated semi-automatic measurement tools. In the landmark-based approach, the height and width of each canal and additional measurements of the common crus were calculated from collected X,Y,Z-Cartesian coordinates of 20 landmarks using basic geometric principles. This provided a total of 10 linear distances.

The semi-automatic measurement in the GOM Inspect program relied on defining a plane interposed into each semicircular canal. These planes were constructed by selecting the surface of the canal and creating objects called "fitting circles." The two methods differed in the treatment of the common crus. While the first approach included the structure, in the second method it was excluded due to its anticipated impact on the slope of the fitting circles.

The measurements included angles measured automatically between canals (more specifically between fitted planes) and the minimum canal lumen dimension (detected automatically in five positions along the curved tube for the first method, and in three positions for the second method). In addition, the second method detected the maximum canal lumens dimension and the height and width of the entire canal arc (using circles circumscribed to the canal cross-sections). To enable the automatic detection of the proposed dimensions, cross-sections at specific points of the semicircular canals and the circles circumscribed and inscribed to these cross-sections were constructed. The minimum and maximum sizes of the canal lumens were estimated as the diameters of these best fitting circles. The two approaches differed in the settings of the radial rasters used for

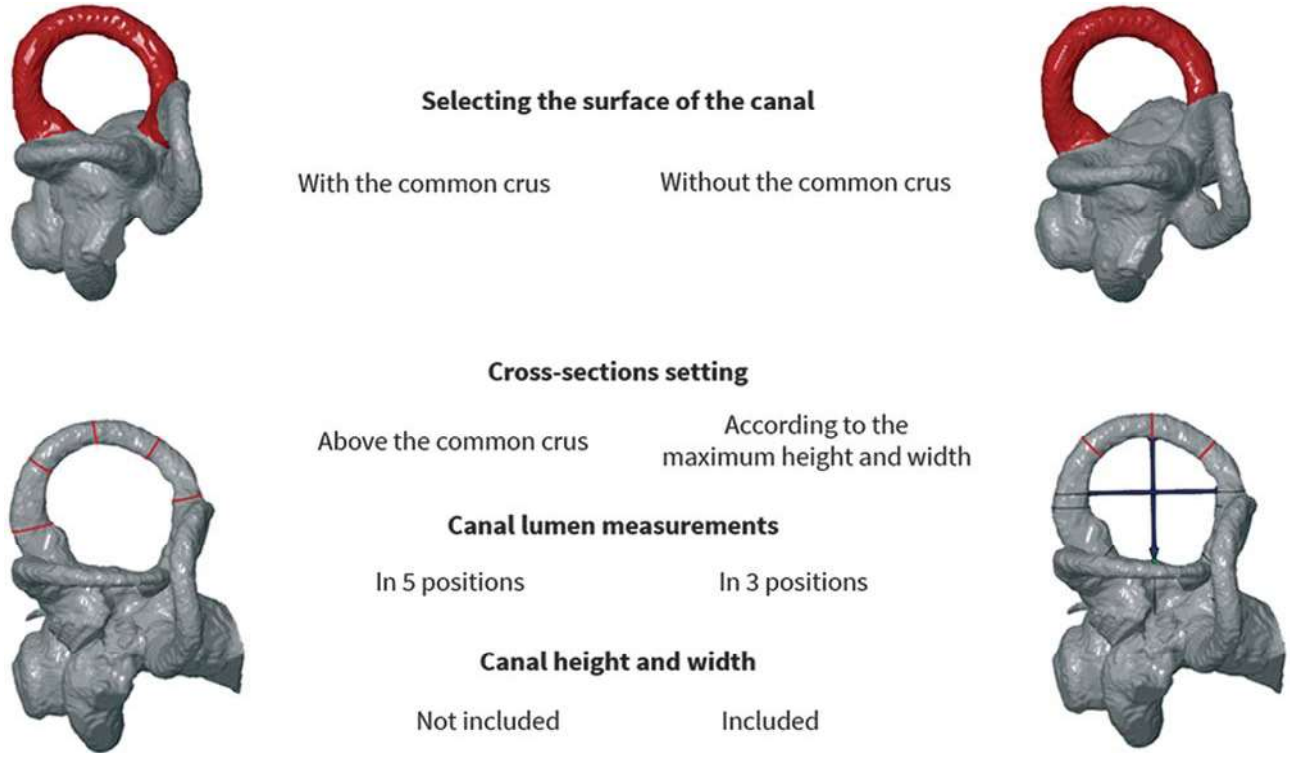

FIGURE 1: Differences between the two measurement procedures in the GOM Inspect program.

construction of the cross-sections. This was the second main difference between the two measurement procedures in the GOM Inspect program. The differences between the two measurement procedures in the GOM Inspect program are depicted in *Figure 1*.

For all three procedures, the intra-observer error was calculated on a sample of twenty randomly selected 3D models. For each measurement protocol, three independent measurements were conducted within a period of one to two weeks. The intra-observer error was expressed in terms of the coefficient of reliability. Based on the values of the coefficients of reliability, the most appropriate data acquisition method was designed, and the most fitting set of measurements was selected by a step-wise elimination procedure. If necessary, further adjustments in the parameter definitions or measurement techniques were made.

Final measurement acquisition procedure

In the first step, the surface of each semicircular canal (including the common crus of the anterior and posterior canal) was selected (*Figure 2*, step 1 – marked red). Then, the plane was fitted into the selected volume of each canal using the Gaussian best-fit method (*Figure 2*, step 2). Subsequently, eight canal cross-sections (each 45° apart) were constructed in accordance with the radial raster by the Multisection Radial function (using "fitting circle" as the Reference Circle, and the center of "fitting circle" as the Starting point). The raster was rotated until a proper position was reached, i.e. perpendicular arms/lines were aligned with the maximum height and width of the canal arc (*Figure 2*, step 3).

In the following steps, the circles with the maximum and minimum size were created for the selected section ellipses using the "Maximum Inscribed Circle" and the "Minimum Circumscribed Circle" function respectively (*Figure 2*, step 5). This was done only for three of the eight constructed cross-sections, as only these ones passed through the arm of the canal itself (not its extended parts) and thus represented the average canal lumen size. This step allowed us to automatically provide the values of the minimum and maximum dimensions of the canal lumen in the given positions. The diameters of each of the constructed circles were determined by the "Check Dimensions – Diameter" function. The three diameters for each canal were averaged. The resulting value of the maximum inscribed circles represented the minimum dimension of the canal lumen, while the average value of the minimum circumscribed circle diameters represented the maximum canal lumen dimension.

The canal width was detected automatically (by the "2-Point Distance" function) as the distance between the centers of two circles circumscribed to the canal cross-sections located in the maximum width of the whole canal (*Figure 2*, step 4). If the common crus of a particular bony labyrinth sample was too high (approx. 10% of the cases), and the crucial cross-section passed through it, then the radial raster (and the associated cross-sections) had to be placed slightly higher. For this reason, a point was constructed in the proper position by the 'Offset Point' function, and employing this point, a circle was created by the "Point-Normal Circle" function. Using these modified elements, new cross-sections of the semicircular canal were constructed, in which the two key arms passed right above the bifurcation of the common crus in the maximum width of the canal (Multisection Radial). The new cross-sections located in the maximum width were used to detect the canal width (again by constructing Minimum Circumsribed Circles and using their centers).

The canal height was also automatically measured using the same function as for the canal width (2-Point Distance). One point used for this detection was the center of the circle circumscribed to the cross-section located at the top of the canal arc/curvature. The opposing point was constructed using the Construct

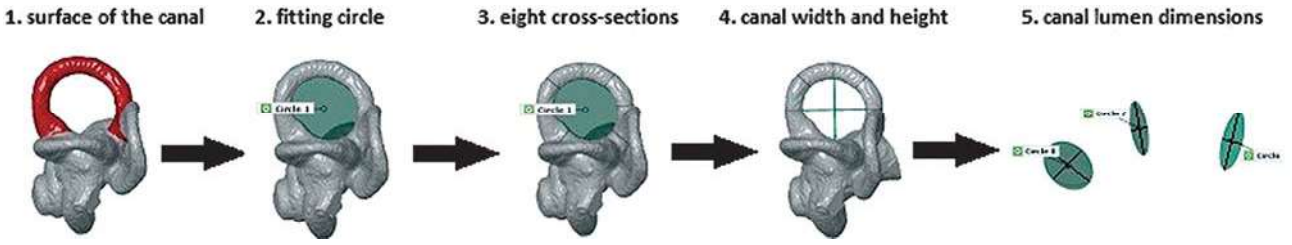

FIGURE 2: Scheme of final measurement acquisition procedure.

Intersection (Normal) With Curved Section function, which enabled the creation of the required point on the edge of the vestibule (the intersection of the "fitting circle" with the cross-section positioned at the bottom of the maximum canal height). In some cases, it was not possible to use this procedure, and the desired point was placed on the edge of the vestibule manually. The canal height was thereafter determined automatically between these two defined points (*Figure 2*, step 4).

The original set of eight linear measurements was taken on each canal – the maximum canal height and width, and the maximum and minimum canal lumen dimension in three positions – was supplemented with five corresponding ratios – the ratio of the maximum canal width to the maximum canal height, the ratio of the average minimum to the average maximum canal lumen dimension, and the ratio of the average maximum canal lumen dimension to the maximum canal height. All of these variables are depicted in *Figure 3*. Their definitions along with abbreviations are listed in *Table 3*.

Morphological study

The technique and set of variables finally selected were employed to quantify morphological variation within the entire studied sample (N=163). The set of distances was tested for dependency on age, sex and laterality. Due to the lack of normal distribution, non-parametric tests were used. The differences between males and females, those between subadults and adults (tested for both sides together as well as for each side independently) and body side-related differences (tested for the entire sample at first, then for the subadults and for the adults independently) were all tested by the Mann-Whitney U test. In addition, side differences at the individual level were tested by the Wilcoxon paired

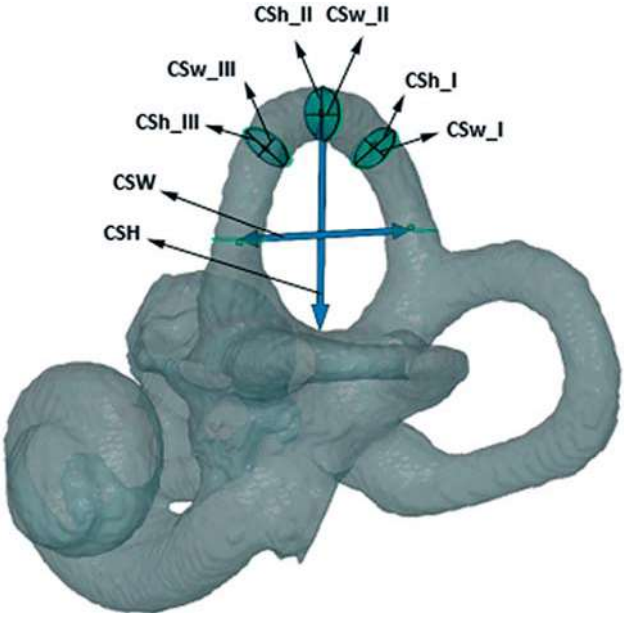

FIGURE 3: The dimensions as measured on the superior semicircular canals.

TABLE 3: The list and the definitions of all parameters.

CSW	maximum width of the whole arc
CSH	maximum height of the whole arc
CSW/CSH	ratio of the maximum width to the maximum height of the whole arc
CSh_I-III	Maximum canal lumen dimension: I: on the cross-section 45° from the location of the maximum canal height toward the common bony crus II: at the location of the maximum height of the whole arc III: on the cross-section 45° from the location of the maximum canal height toward the ampullary bony crus
CSh	Average maximum canal lumen dimension (computed as the average of maximum canal lumen dimensions measured in three positions – CSmax_I-III)
CSw_I-III	Minimum canal lumen dimension: I: on the cross-section 45° from the location of the maximum canal height toward the common bony crus II: at the location of the maximum height of the whole arc III: on the cross-section 45° from the location of the maximum canal height toward the ampullary bony crus
CSw	Average minimum canal lumen dimension (computed as the average of minimum canal lumen dimensions measured in three positions – CSmin_I-III)
CSw/CSh	Ratio of the average minimum to average maximum canal lumen dimension
CSh/CSH	Ratio of the average maximum canal lumen dimension to the height of the whole arc

test. The age changes between the seven defined age categories were tested by the Kruskal-Wallis analysis of variance. If not stated otherwise, all the tests were carried out in STATISTICA 12 (StatSoft. Inc. 2013) at a 5% level of significance. Intraclass correlation coefficients were calculated in MedCalc software (Medcalc.org 2020) for different sets of dimensions as shown in *Table 4*, by two-way model – the same raters for all subjects, type consistency.

RESULTS

Intra-observer error

In general, the values of the coefficients of reliability acquired for the angular measurements varied significantly (0.56–0.99). Therefore, these parameters were the first excluded from the pool of suitable measurements. Measurements of the canal heights and widths, acquired in the second method in the GOM Inspect program, were higher than 0.95 for all the canals. In comparison, the values of the corresponding dimensions detected in the Landmark program were in the interval from 0.84 to 0.98. The coefficients of reliability for almost all the dimensions were lower using the landmark-based approach than using the GOM Inspect program (the only exception to this was the lateral canal height, which had a value of 0.98 for both techniques). For the anterior and posterior canal, the dimensions measured on the canal lumens exhibited very high values (more than 0.97) in both GOM protocols. However, the values were a little lower for the lateral canal in both procedures (with one exception more than 0.85). The results showed that more consistent measurements were achieved with the automatic tools incorporated in the GOM Inspect program.

Morphological study

Sex-related differences were revealed only for a single measurement: CSAw – the average minimum dimension of the anterior canal lumen (p-value = 0.018). Furthermore, the Mann-Whitney U test showed no statistically significant side-specific differences. The Wilcox paired test showed that statistically significant differences between right and left sides at the individual level were present in two variables – one maximum dimension on the posterior canal (CSPh_III; p-value = 0.024) for all individuals, and one maximum dimension on the anterior canal (CSAh_I; p-value = 0.041) for the adult specimens.

No statistically significant differences were shown among age categories in any of the measurements. Statistically significant differences between subadults and adults regardless of the side specification were demonstrated primarily in the dimensions of the canal lumen, except for the height dimensions of the anterior

TABLE 4: Result of intraclass correlation coefficient analysis.

		Intraclass correlation	**95% Confidence Interval**
CSLh: positions I–III	single measures	0.753	0.681 to 0.814
CSLw: positions I–III	single measures	0.800	0.738 to 0.851
CSAh: positions I–III	single measures	0.837	0.764 to 0.893
CSAw: positions I–III	single measures	0.847	0.777 to 0.900
CSPh: positions I–III	single measures	0.736	0.645 to 0.812
CSPw: positions I–III	single measures	0.794	0.719 to 0.855
CShI: L, A, P	single measures	0.461	0.297 to 0.616
CSwI: L, A, P	single measures	0.646	0.510 to 0.761
CShII: L, A, P	single measures	0.551	0.415 to 0.674
CSwII: L, A, P	single measures	0.569	0.434 to 0.691
CShIII: L, A, P	single measures	0.417	0.284 to 0.547
CSwIII: L, A, P	single measures	0.500	0.374 to 0.619
CSh: L, A, P	average measures	0.793	0.718 to 0.851
CSw: L, A, P	average measures	0.814	0.747 to 0.866
CSH: L, A, P	single measures	0.550	0.414 to 0.674
CSW: L, A, P	single measures	0.557	0.421 to 0.680

canal. The highest statistically significant difference between subadults and adults was detected in the posterior canal, specifically in the ratio of the average maximum canal lumen dimension to the canal height (CSh/CSH).

If tested separately, the right-sided labyrinths were shown to be more dimorphic (considering the lateral and posterior canals lumen) than their left-sided counterparts. The most statistically significant difference for the right-sided labyrinths was yielded in the same parameter (the ratio of the average maximum canal lumen dimension relative to the canal height in the posterior canal (CSh/CSH)) as for both sides together. No statistically significant differences in the anterior canal were revealed either on the right or on the left side. In regard to the size of the entire canal arcs, the width of the left-sided lateral canal showed statistically significant differences (*Table 5*).

DISCUSSION

The human bony labyrinth has been an object of interest in physical anthropology for a long time. This is mainly due to the high degree of preservation of this structure, located as it is in the hardest and toughest bone of the human body. However, this great advantage is at the same time a disadvantage, since it makes this structure difficult to examine.

One solution to this problem has come with the development of digital technologies and their implementation in physical anthropology. Volume scanning, in particular, contributes greatly to research of inner structures such as the bony labyrinth, which are difficult to access and therefore have been explored insufficiently. Three-dimensional virtual models, which can be generated from volumetric data, provide many new possibilities for assessment. First, digital models are a permanent record of a structure's morphology, and thus they can be archived, revised, repeatedly evaluated, and shared. Three-dimensional specimens also offer more complex spatial information than two-dimensional images, and this makes an exhaustive analysis of a structure's geometry much easier. Besides that, digital models reveal previously concealed traits/features, which can be helpful in clarifying discrepancies in the results of morphometric studies (Weber *et al.* 2001, Weber 2015).

However, it is necessary to take into account that accuracy of such three-dimensional models and

TABLE 5: The results of testing the differences between subadult and adult individuals (regardless of the side and for the right and the left side separately) by Mann-Whitney nonparametric test.

	Subadult and adult individuals								
	Both sides	**Right side**	**Left side**	**Both sides**	**Right side**	**Left side**	**Both sides**	**Right side**	**Left side**
	p-value	**p-value**	**p-value**	**p-value**	**p-value**	**p-value**	**p-value**	**p-value**	**p-value**
		L			**A**			**P**	
CSW	0.165	0.805	**0.046**	0.434	0.930	0.333	0.859	0.559	0.416
CSH	0.503	0.640	0.173	0.143	0.557	0.134	0.478	0.518	0.620
CSW/CSH	0.419	0.693	0.141	0.655	0.539	0.964	0.184	0.124	0.617
CSh_I	0.074	**0.042**	0.661	0.168	0.064	0.803	**0.007**	0.072	**0.032**
CSh_II	**0.027**	0.123	0.107	0.065	0.096	0.331	**0.028**	**0.037**	0.295
CSh_III	0.135	0.201	0.490	0.112	0.437	0.170	**0.004**	**0.026**	0.090
CSh	**0.021**	**0.047**	0.256	0.149	0.358	0.329	**0.007**	**0.046**	0.100
CSw_I	**0.003**	**0.031**	0.051	0.131	0.136	0.548	**0.017**	0.079	0.120
CSw_II	0.124	0.240	0.361	**0.044**	0.114	0.242	**0.010**	**0.013**	0.237
CSw_III	0.080	0.115	0.350	**0.009**	0.077	0.050	0.128	0.139	0.572
CSw	**0.020**	0.077	0.126	0.116	0.210	0.342	0.209	0.329	0.529
CSw/CSh	0.254	0.733	0.282	0.265	0.412	0.406	0.084	0.503	0.085
CSh/CSH	0.676	0.320	0.707	0.612	0.695	0.771	**0.000**	**0.002**	0.080

associated feasibility and accuracy of their quantification is highly affected by the slice thickness of CT data. Comparison of the three-dimensional reconstructions created from CT data with different slice thicknesses (0.625–5 mm) has shown that loss, incompleteness or fusion of certain structures, features or specific sections occurred when the thicknesses were the highest (2–5 mm). This points to the need for setting specific imaging protocols regarding data capturing and their 3D reconstructions to ensure their sufficiency for the required analysis (Ford, Decker 2016).

Due to the intricate architecture of the bony labyrinth, it is extremely difficult to define its dimensions with sufficient accuracy and detail. Existing definitions of parameters do not always meet these requirements (Osipov *et al.* 2013). The wide range of variations of the studied components, in particular, makes it very challenging to formulate a clear and indisputable interpretation of any one parameter's definition. Furthermore, the effect of the structure's position and orientation relative to the observing researcher on the resulting measurements is regarded as greatly problematic. In contrast, working with virtual models enables a more accurate examination of the structures, since the model can be freely positioned and rotated, and thus the dimensions can be inspected from every viewpoint during measuring. Virtual models also enable the assessment of otherwise inaccessible dimensions (Weber 2015), and making it easier to develop novel evaluation methods in which some steps can be automated.

In this paper, one method based on landmarks collected manually in the Landmark program and two semiautomatic procedures of measurement conducted in GOM Inspect program were devised and tested. Repeated test measurements showed that the landmark-based method exhibited the poorest rates of accuracy and repeatability. For this reason, this approach was abandoned relatively early in the analysis. We do not recommend using the landmark-based method in studies exploring variations of the human bony labyrinth.

In contrast, the semi-automatic measurement showed that it could provide consistent results. Both semiautomatic procedures used the wide functionality of the GOM Inspect program to reduce the potential for error caused by the sample's placement and orientation in space during measurement. The program enabled the construction of geometric objects representing certain structures of the bony labyrinth. These geometric objects were given selected characteristics corresponding to the target dimensions. The program allowed these characteristics (and thus the target dimensions) to be measured automatically.

Overall, the designed measurement methods using the GOM Inspect program proved very suitable for assessment of the bony labyrinth. However, one part of the procedure, the creation of fitting circles, turned out to be problematic. The angles between semicircular canals were detected automatically using "fitting circles," but the accuracy and repeatability of this step was poor. Small differences resulting from repeated manual selection of the semicircular canal area had a significant effect on the resulting inclination of the "fitting circle" defining the canal plane. The selection of the lateral canal area was particularly tricky, as its border was often undefined. Therefore, we can conclude that the proposed approach is not suitable for angular measurement, unless the area of the canals (particularly the boundary of their origin) is defined well enough to yield a higher accuracy in the measurements. Although other steps of the protocol also utilized "fitting circles," the inclination of the circles evidently did not affect them significantly, as the acquired coefficients of reliability were very high for all the detected parameters in these steps.

The morphometric analysis of the human bony labyrinth in our study revealed no side variations when the overall size of the structure was taken into account. The same results were reported in the majority of previous research (Lee *et al.* 2013, Della Santina *et al.* 2005, Hardy 1938). However, Osipov *et al.* (2013) observed notable side differences in their study, including many of the analyzed parameters on the cochlea, anterior and posterior canals. Regarding the canal lumen size, our sample showed some very small side-related morphological variations when employing pairwise comparison. Nonetheless, this disparity concerned only two parameters, in both cases the height dimensions. In the only other study including evaluation of the canal lumen (Lee *et al.* 2013), no side differences were found. It should be mentioned, however, that the measured parameters (canal lumen heights and widths) were not entirely corresponding, which could also affect the comparison. In our study these parameters were represented by the maximum and the minimum dimension of the canal lumen, and did not necessarily have to be perpendicular. This contrasts with the study by Lee *et al.* (2013), in which they had to be perpendicular.

The evaluation of sexual dimorphism yielded similarly ambiguous results. With respect to the canal

lumen size, a very low degree of sexual dimorphism was observed. Only one of the measured parameters was statistically significant, which is almost negligible when considering the overall sexual dimorphism. In Lee *et al.* (2013) no sex differences were detected, although it is again necessary to take into account the aforementioned differences between the definitions of the dimensions in this case. When regarding the overall canal size, only minimum sex differences were found in Marcus *et al.* (2013), and none in Lee *et al.* (2013). This is consistent with our results. In contrast, Osipov *et al.* (2013) observed a very high degree of sexual dimorphism. The differences were found in all heights and widths of the semicircular canals, and a method for sex estimation was even devised based on these parameters, with 80% of cases correctly classified. Sato *et al.* (1991) also detected a high degree of sexual dimorphism, around 12.9%. If accurate, this would be a larger inter-sex difference than for any other cranial metric feature reported in the human skull (Urbanová *et al.* 2013a, b), and it would put the feature in the same category of highly sexual dimorphic sites as, for instance, the mastoid process (Urbanová 2009).

It is generally accepted that the human bony labyrinth acquires its adult morphology before birth. This assumption is based on findings that show that the development of this structure is completed by the end of the second or the beginning of the third trimester (Richard *et al.* 2010, Jeffery, Spoor 2004), and was confirmed also by studies in which no age differences were found (Sato *et al.* 1991, Mori, Chang 2012, Jeffery, Spoor 2004). Although no statistically significant differences between different age categories were found in the present study, they were detected between the groups of adult and subadult individuals in many variables. Most of the concerned variables occurred on the lateral and posterior canal. In contrast, on the anterior canal, the differences were significantly less evident. However, this finding did not necessarily reflect the lower degree of dimorphism on the anterior canal. This result might also be due to poor preservation of this canal in many of the studied samples, which made it difficult or impossible to acquire some of its dimensions, thus lowering the number of parameters available for analysis.

The morphological differences were observed again exclusively in the canal lumen size, with only one exception, the overall width of the lateral canal. As the values were higher for adults in most of the cases, it may be that the bone around the semicircular canals is resorbed with increasing age, which leads to the widening of the canal lumen. According to our results, it can be assumed that whereas the overall size of the human bony labyrinth does not change during the postnatal development, some modifications occur in the size of the canal lumen. Bone tissue is constantly being remodeled. In adults, this allows the bony elements to modify their morphology to a certain extent. An analogy to this process in the semicircular canals could be age-related medullary cavity extension (Acsádi, Nemeskéri 1970) or enlargement of Haversian canals (Harrison, Cooper 2015). Since the evaluation of age differences of the canal lumen was not included in any other paper, we can neither disprove nor confirm this assumption.

Generally, it can be said that the methods using the GOM Inspect program proposed in this study are appropriate for the morphometric analysis of the human bony labyrinth, since sufficient accuracy and repeatability of the measurements was demonstrated.

CONCLUSION

The procedure developed in this study is a fine example of the potential of non-invasive examination. This method represents a novel and accurate option for assessing spatially complex and inaccessible structures such as the bony labyrinth. The proposed method includes automatic steps, which makes assessment more accurate and can help reduce the possibility for error arising from the position of the model during measurement. Further, it enables a detailed analysis of the semicircular canal lumen, which has not been included in the previous studies.

The results show almost no age-, sex- or side-differences when analyzing the overall size of the semicircular canals. Nevertheless, some statistically significant differences were revealed between adults and subadults in the canal lumen size (mainly on the lateral and posterior one), indicating that these parts can change to a certain extent during life. Unfortunately, these findings have little to no practical use while assessing a biological profile from skeletal remains. Nevertheless, they shed light on some interesting morphological variations of the human bony labyrinth.

ACKNOWLEDGMENTS

The study was carried out with a financial support provided by Project Grant at Masaryk University, project No. MUNI/A/1219/2016 and MUNI/A/1198/2017.

REFERENCES

ACSÁDI G., NEMESKÉRI J., 1970: *History of human life span and mortality*. Budapest: Akadémiai Kiadó.

BECKETT R. G., CONLOGUE G. J., 2010: Paleoimaging: *Field applications for cultural remains and artefacts.* Boca Raton, Florida, USA: CRC Press (Taylor & Francis).

DELLA SANTINA C. C., POTYAGAYLO V., MIGLIACCIO A., MINOR L. B., CAREY J. P., 2005: Orientation of Human Semicircular Canals Measured by Three-Dimensional Multiplanar CT Reconstruction. *Journal of the Association for Research in Otolaryngology* 6: 191–206. doi: 10.1007/s10162-005-0003-x

DOKLÁDAL M., PÁČ L., 2000: *Anatomie člověka III.* Brno: Masarykova univerzita.

DORLAND, W. A. N., 2011: *Dorland's illustrated medical dictionary. 32nd Ed.* Philadelphia: Elevier Saunders.

FORD J. M., DECKER S. M., 2016: Computed tomography slice thickness and its effects on three-dimensional reconstruction of anatomical structures. *Journal of Forensic Radiology and Imaging* 4: 43–46. doi: 10.1016/j.jofri.2015.10.004

GOM mBH., 2013: *GOM Inspect*, Version 1.2.1.

GUNZ P., RAMSIER M., KUHRIG M., HUBLIN J. J., SPOOR F., 2012: The mammalian bony labyrinth reconsidered, introducing a comprehensive geometric morphometric approach. *Journal of Anatomy* 220: 529–543. doi: 10.1111/j.1469-7580.2012.01493.x

HAMMER Ø., HARPER D. A. T., RYAN P. D., 2001: PAST, *Paleontological Statistics Software Package for Education and Data Analysis*. Palaeontologia Electronica 4, 1: 9.

HARDY M., 1938: The length of the organ of Corti in man. *American Journal of Anatomy* 62, 2: 291–311. doi: 10.1002/aja.1000620204

HARRISON K. D., COOPER D. M., 2015: Modalities for visualization of cortical bone remodeling: the past, present and future. *Frontiers in Endocrinology* 6: 122. doi: 10.3389/fendo.2015.00122.

HENDERSON E., WILKINS A., HUANG L., KENNA M., GOPEN Q., 2011: Histopathologic investigation of the dimensions of the cochlear nerve canal in normal temporal bones. *International Journal of Pediatric Otorhinolaryngology* 75, 4: 464–467. doi: 10.1016/j.ijporl.2010.11.024

ImageConverter Plus, 2003–2009: fCoder Group, Inc., version 8.0. 174.

JEFFERY N., SPOOR F., 2004: Prenatal growth and development of the modern human labyrinth. *Journal of Anatomy* 204, 2: 71–92. doi: 10.1111/j.1469-7580.2004.00250.x

JUNGEROVÁ J., KRÁLÍK M., FOJTÍK P., URBANOVÁ P., 2016: Základní antropologická analýza kosterních pozůstatků z mladohradištního pohřebiště v Dětkovicích - Za zahradama (okr. Prostějov). *Pravěk NŘ* 24: 253–264.

KOVÁČOVÁ V., JUNGEROVÁ J., URBANOVÁ P., VLAHOVÁ V., RYVOLOVÁ M., VACULOVIČOVÁ M., KRÁLÍK M., 2016: The assessment of the semicircular canals and cochlea of the human bony labyrinth using imaging techniques. *20th Congress of the European Anthropological Association, 24.–28. 8. 2016, Zagreb, Croatia*. 2016.

LEE J. Y., SHIN K. J., KIM J. N., YOO J. Y., SONG W. CH., KOH K. S., 2013: A Morphometric Study of the Semicircular Canals Using Micro-CT Images in Three-Dimensional Reconstruction. *The Anatomical Record* 296: 834–839. doi: 10.1002/ar.22664

MARCUS S., WHITLOW C. T., KOONCE J., ZAPADKA M. E., CHEN M. Y., WILLIAMS D. W. 3RD, LEWIS M., EVANS A. K., 2013: Computed tomography supports histopathologic evidence of vestibulocochlear sexual dimorphism. *International Journal of Pediatric Otorhinolaryngology* 77: 1118–1122. doi: 10.1016/j.ijporl.2013.04.013

MedCalc Statistical Software, 2020: *MedCalc Software Ltd*, Ostend, Belgium, version 19.2.1, https://www.medcalc.org.

MORI M. C., CHANG K. W., 2012: CT Analysis Demonstrates That Cochlear Height Does Not Change with Age. *American Journal of Neuroradiology* 33: 119–123. doi: 10.3174/ajnr.A2713

MÜLLER R., 2009: Hierarchical microimaging of bone structure and function. *Nature Reviews. Rheumatology* 5,7: 373–381. doi: 10.1038/nrrheum.2009.107.

OSIPOV B., HARVATI K., NATHENA D., SPANAKIS K., KARANTANAS A., KRANIOTI, E. F., 2013: Sexual Dimorphism of the Bony Labyrinth: Applications in Forensic Anthropology and Osteoarchaeology. *American Journal of Physical Anthropology* 151: 290–301. doi: 10.1002/ajpa.22279

RECHEIS W., WEBER G. W., SCHAFER K., KNAPP R., SEIDLER H., ZUR NEDDEN D., 1999a: Virtual reality and anthropology. *European Journal of Radiology* 31: 88–96. doi: 10.1016/S0720-048X(99)00089-3

RICHARD C., LAROCHE N., MALAVAL L., DUMOLLARD J. M., MARTIN, CH., PEOCH M., VICO L., PRADES, J. M., 2010: New insight into the bony labyrinth: A microcomputed tomography study. *Auris Nasus Larynx* 37: 155–161. doi: 10.1016/j.anl.2009.04.014

SATO H., SANDO I., TAKAHASHI H., 1991: Sexual dimorphism and development of the human cochlea. Computer 3-D measurement. *Acta oto-laryngologica* 111, 6: 1037–1040. doi: 10.3109/00016489109100753

SATO H., SANDO I., TAKAHASHI H., 1992: Computer-aided three-dimensional measurement of the human vestibular apparatus. *Otolaryngology-Head and Neck Surgery* 107: 405–459. doi: 10.1177/019459989210700311

SPOOR F., JEFFERY N., ZONNEVELD F., 2000: Using diagnostic radiology in human evolutionary studies. *Journal of anatomy* 197: 61–76. doi: 10.1046/j.1469-7580.2000.19710061.x

StatSoft, Inc., 2013: STATISTICA (data analysis software system), Version 12.0. www.statsoft.com.

URBANOVÁ, P., 2009: *A Study of Human Craniofacial Variation by Using Geometric Morphometrics* (Dissertation thesis). Brno: Masaryk University, Faculty of Science, Department of Anthropology.

URBANOVÁ P., HEJNA P., ZÁTOPKOVÁ L., ŠAFR M., 2013: The morphology of human hyoid bone in relation to sex, age and body proportions. *HOMO - Journal of Comparative Human Biology* 64,3: 190–204. doi: 10.1016/j.jchb.2013.03.005

URBANOVÁ, P., HEJNA, P., ZÁTOPKOVÁ, L., ŠAFR, M., 2013: What is the appropriate approach in sex determination of hyoid bones? *Journal of Forensic and Legal Medicine* 20, 8: 996–1003. doi: 10.1016/j.jflm.2013.08.010

Visage Imaging, Inc., 2010: *Amira*, Version 5.3.2.

WEBER G. W., SCHAEFER K., PROSSINGER H., GUNZ P., MITTEROECKER P., SEIDLER H., 2001: Virtual anthropology: the digital evolution in anthropological sciences. *Journal of Physiological Anthropology and Applied Human Science* 20: 69–80. doi: 10.2114/jpa.20.69

WEBER G., 2015: Virtual anthropology. *American Journal of Physical Anthropology* 156: 22–42. doi: 10.1002/ajpa.22658

WILEY, D. F., 2002–2005: Institute for Data Analysis and Visualization (IDAV). *Landmark,* Version 3.0.

Veronika Kováčová*
Petra Urbanová
Laboratory of Morphology and Forensic Anthropology
Department of Anthropology
Faculty of Science, Masaryk University
Kotlářská 2, 611 37 Brno
Czech Republic
E-mail: kovacova.v@mail.muni.cz
E-mail: urbanova@sci.muni.cz

*Corresponding author.